SUPPLEMENTAL MATERIAL

Nonequilibrium dark space phase transition

Federico Carollo[1] and Igor Lesanovsky[1,2]

[1] *Institut für Theoretische Physik, Universität Tübingen, Auf der Morgenstelle 14, 72076 Tübingen, Germany*
[2] *School of Physics and Astronomy and Centre for the Mathematics and Theoretical Physics of Quantum Non-Equilibrium Systems, The University of Nottingham, Nottingham, NG7 2RD, United Kingdom*

ANALYTICAL AND NUMERICAL METHODS

Infinite-dimensional lattice

In an infinite-dimensional lattice, each site has, as nearest neighbors, all the remaining ones forming the many-body system. As stated in the main text, this results in a constraint $\Pi^k_\bullet$ of the form given in Eq. (5). Therefore, the dynamics of the average quantum state can be described through the quantum master equation (1), with a Hamiltonian given by

$$H \approx \Omega_1 \sum_{k=1}^{N} \lambda_1^{(k)} + \frac{\Omega_2}{N} \sum_{k,h=1}^{N} n_\bullet^{(h)} \lambda_6^{(k)} \,. \tag{S1}$$

The approximation is just due to the fact that we have added terms with $k = h$ in the double sum. In the limit $N \to \infty$, this does not constitute a problem, since these terms give rise to an intensive Hamiltonian contribution, irrelevant for the dynamics of the system observables.

In order to investigate the stationary behavior of the model, we focus on collective operators describing "sample-average" properties. We consider

$$P_\alpha = \frac{1}{N} \sum_{k=1}^{N} n_\alpha^{(k)} \,, \quad \text{with } \alpha = \bullet, *, \circ \,, \tag{S2}$$

representing the density of sites in the different states, as well as

$$G_\alpha = \frac{1}{N} \sum_{k=1}^{N} \lambda_\alpha^{(k)} \,, \quad \text{for } \alpha = 1, 2, 4, 5, 6, 7 \,. \tag{S3}$$

We stress here that we are using the Gell-Mann matrices λ_α for off-diagonal single-site observables, while we use the projectors n_α for the diagonal ones.

Average Lindblad Dynamics

The collective operators of Eqs. (S2)-(S3) behave, when considering the state $|\mathrm{U}\rangle$ and the large N limit, as "classical" scalar quantities equal to their expectation value on the state [22]. This means that we have $G_\alpha \to \Lambda_\alpha = \langle \lambda_\alpha \rangle$ as well as $P_\alpha \to \varrho_\alpha = \langle n_\alpha \rangle$, where we have also exploited the translation invariance of the state. For the infinite-dimensional

lattice, the dynamics of these operators is captured by the following non-linear differential equations [19] ($\partial_t := d/dt$)

$$\begin{aligned}
\partial_t\Lambda_1 &= \Omega_2\varrho_\bullet\Lambda_5 - \Omega_2\Lambda_2\Lambda_6 - \frac{\gamma}{2}\Lambda_1\,,\\
\partial_t\Lambda_2 &= -2\Omega_1(\varrho_\bullet - \varrho_*) - \Omega_2\varrho_\bullet\Lambda_4 + \Omega_2\Lambda_1\Lambda_6 - \frac{\gamma}{2}\Lambda_2\,,\\
\partial_t\Lambda_4 &= -\Omega_1\Lambda_7 + \Omega_2\varrho_\bullet\Lambda_2 - \Omega_2\Lambda_5\Lambda_6\,,\\
\partial_t\Lambda_5 &= \Omega_1\Lambda_6 - \Omega_2\varrho_\bullet\Lambda_1 + \Omega_2\Lambda_4\Lambda_6\,,\\
\partial_t\Lambda_6 &= -\Omega_1\Lambda_5 - \frac{\gamma}{2}\Lambda_6\,,\\
\partial_t\Lambda_7 &= \Omega_1\Lambda_4 - 2\Omega_2\varrho_\bullet(\varrho_* - \varrho_\circ) - \frac{\gamma}{2}\Lambda_7\,,\\
\partial_t\varrho_\bullet &= \Omega_1\Lambda_2\,,\\
\partial_t\varrho_* &= -\Omega_1\Lambda_2 + \Omega_2\varrho_\bullet\Lambda_7 - \gamma\varrho_*\,,\\
\partial_t\varrho_\circ &= -\Omega_2\varrho_\bullet\Lambda_7 + \gamma\varrho_*\,.
\end{aligned} \tag{S4}$$

To find the possible stationary states, we set to zero all the time-derivatives above. In this way, we find the following three solutions:

$$\begin{array}{ccc}
\varrho_\bullet = 0, & \varrho_\circ = 1, & \Lambda_4 = 0;\\
\varrho_\bullet = \frac{1}{2}\left[1-\sqrt{1-x^2}\right], & \varrho_\circ = \frac{1}{2}\left[1+\sqrt{1-x^2}\right], & \Lambda_4 = -x;\\
\varrho_\bullet = \frac{1}{2}\left[1+\sqrt{1-x^2}\right], & \varrho_\circ = \frac{1}{2}\left[1-\sqrt{1-x^2}\right], & \Lambda_4 = -x;
\end{array}$$

with $x = 2\Omega_1/\Omega_2$ and all other collective quantities being zero. The last two solutions are physically meaningful only for $|x| \leq 1$. This shows the existence of a critical rate $\Omega_2^{\rm c} = 2\Omega_1$ below which the unique admissible solution is the first one, which is the exact dark state $|{\rm D}\rangle$. When $\Omega_2 \geq \Omega_2^{\rm c}$ ($|x| \leq 1$), two further solutions become possible. The second one turns out to be unstable so that it is never dynamically approached. The third, instead, corresponds to a (stable) emergent stationary state with a finite density of sites in $|\bullet\rangle$. This state is pure and, concerning the computation of local observables or of collective operators such as those introduced before, can be represented as the state

$$|{\rm D_e}\rangle = \bigotimes_{k=1}^{N}\left(\alpha_+\,|\bullet\rangle - \alpha_-\,|\circ\rangle\right)^{(k)}\,, \tag{S5}$$

with $\alpha_\pm = \sqrt{2}^{-1}\sqrt{1\pm\sqrt{1-x^2}}$. However, due to the all-to-all coupling in the Hamiltonian of Eq. (S1), the state $|{\rm D_e}\rangle$ can develop weak long-range correlations [19, 25, 26], as shown in the last subsection of this section. In order to verify which stationary state is dynamically approached when the system is initially in $|{\rm U}\rangle$, we have performed a numerical integration of Eqs. (S4), up to large times for which the state is stationary. These results are presented in Fig. 2(a-b) in the main text.

Exact diagonalization of the effective Hamiltonian

To show that the emergent dark state is approached through the dynamics of Eq. (4), we have performed exact diagonalization of the non-Hermitean Hamiltonian $H_{\rm eff}$. The idea is that since the emergent stationary state $|{\rm D_e}\rangle$ is pure, it must be, in the $N\to\infty$ limit, an eigenvector of $H_{\rm eff}$ associated with a second eigenvalue which converges to zero in imaginary part. In this way, the rate of escaping from $|{\rm D_e}\rangle$ would be zero and the dynamics in Eq. (4) would have this state as a possible fixed point. Since we start from the fully symmetric state $|{\rm U}\rangle$, and since the average Lindblad dynamics is fully symmetric (invariant under any permutation of the three-level units), in order to detect the emergence of the second dark state $|{\rm D_e}\rangle$, it is sufficient to diagonalize the effective Hamiltonian in its fully symmetric subspace. To do so, we have developed a representation of such an operator in the space of vectors which are invariant under any permutation of two subsystems. Such a subspace can be constructed, for instance, by acting on the fully symmetric vector $|{\rm U}\rangle$ with permutation invariant operators. The procedure to obtain such a representation of the effective Hamiltonian is presented in a following section.

Quantum correlations in the emergent dark state

Due to the collective nature of the model in the infinite-dimensional geometry, the emergent dark state reduces to the uncorrelated state introduced in Eq. (S5) whenever local or average quantities are considered. However,

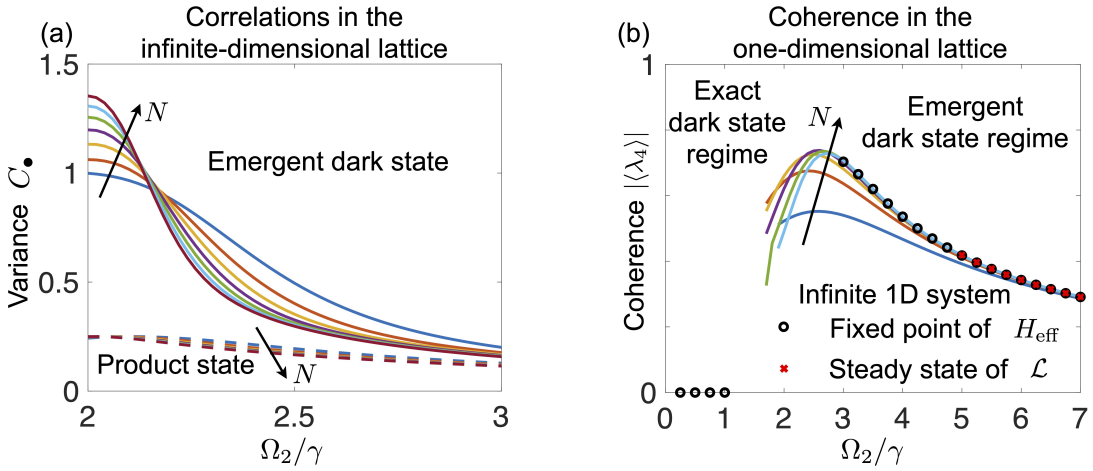

FIG. S1. **Correlations and coherence in the emergent dark state**. (a) Plot of the variance of the number of contagious sites in the emergent dark state, for the infinite-dimensional lattice. We have set $\Omega_1 = 1$ (in units of γ). The variance is computed for the eigenvector of $H_{\rm eff}$ associated with the gap of the Lindblad generator, for $N = 20, 30, \dots 80$ (solid lines). The dashed lines, report, for the same system sizes, the variance of the order parameter for a translation invariant product state with same value of the order parameter of the emergent dark state. The difference between these sets of curves demonstrates that the emergent dark state features quantum correlations. (b) Plot of the coherence $|\langle\lambda_4\rangle|$ for the one-dimensional lattice, with $\Omega_1 = 1$ (in units of γ). Solid lines are obtained from the eigenvector of $H_{\rm eff}$ associated with the gap for $N = 3, 4, \dots 8$. Black circles represent the same quantity estimated from MPS algorithms for the system in the thermodynamic limit. Red crosses represent instead the value of the coherence in the stationary state of the Lindblad dynamics $\mathcal{L}$. These numerical results demonstrate that the emergent dark state retains quantum coherence.

it is possible to show that the emergent dark state displays collective quantum correlations. In this section, we demonstrate this by considering collective observables (see also discussion in [25, 26]), as for instance encoded in the variance of the total number operator of the contagious sites, see Eq. (S6) below.

We focus here on the variance of the operator $\sum_{k=1}^{N} n_\bullet^{(k)}$ defined as

$$C_\bullet = \frac{1}{N}\sum_{k,h=1}^{N}\left(\langle n_\bullet^{(k)} n_\bullet^{(h)}\rangle - \langle n_\bullet^{(k)}\rangle\langle n_\bullet^{(h)}\rangle\right); \tag{S6}$$

the quantity above can be seen as a susceptibility for the order parameter $\rho_\bullet$. Now, we make the following consideration. If the state $|\mathrm{D}_\mathrm{e}\rangle$ was in a product state form, one would have that $\langle n_\bullet^{(k)} n_\bullet^{(h)}\rangle = \langle n_\bullet^{(k)}\rangle\langle n_\bullet^{(h)}\rangle$ for $k \neq h$. In this case, the variance $C_\bullet$ would be equal to

$$C_\bullet^{\rm prod} = \rho_\bullet(1-\rho_\bullet)\,.$$

In Fig. S1(a), we show that the numerically computed variance in the emergent dark state is different from the one that one would find for a product state characterized by the same value of the order parameter. This demonstrates that $|\mathrm{D}_\mathrm{e}\rangle$ cannot be in a product state, and since it is pure, it must be a state featuring quantum correlations. These correlations cannot be detected by looking at local or average observables and are thus collective in nature such as those described in [19, 25, 26] through quantum fluctuations.

One-dimensional lattice: simulations with matrix product states

Effective Hamiltonian dynamics

For the one-dimensional lattice, to investigate the transition from the dark state $|\mathrm{D}\rangle$ to the dark state $|\mathrm{D}_\mathrm{e}\rangle$, we use a time-evolving-block-decimation algorithm (TEBD) which exploits the translation invariance of the model to address the system in the infinite one-dimensional lattice limit (iTEBD), see Refs. [27–30] for details. Since we cannot perform exact diagonalization of $H_{\rm eff}$, we analyze the fixed point obtained by running the dynamics in Eq. (4), starting from state $|\mathrm{U}\rangle$, for sufficiently large times.

The formal integration of Eq. (4) gives the solution

$$|\psi_t\rangle = \frac{W_t\,|\psi\rangle}{\|W_t\,|\psi\rangle\,\|}\,,$$

where the time-propagator is given by $W_t = e^{-\mathrm{i}tH_{\mathrm{eff}}}$. In order to simulate such dynamics by means of matrix product state (MPS) methods, we first discretize time. We take a sufficiently small time step dt and express the infinitesimal propagator W_{dt} through the second-order Trotter decomposition

$$W_{dt} \approx e^{-\mathrm{i}dt/2H_{\mathrm{ss}}}e^{-\mathrm{i}dt/2H_{\mathrm{o}}}e^{-\mathrm{i}dtH_{\mathrm{e}}}e^{-\mathrm{i}dt/2H_{\mathrm{o}}}e^{-\mathrm{i}dt/2H_{\mathrm{ss}}}\,,$$

where $H_{\mathrm{ss}} = \sum_k(\Omega_1\lambda_1^{(k)} - \mathrm{i}\gamma/2n_*^{(k)})$ is the single-site component of the effective Hamiltonian, while $H_{\mathrm{o/e}}$ contain the nearest-neighbor interaction terms for odd and even bonds, respectively.

We perform time updates for the MPS representation of the state $|\psi_t\rangle$, using a standard iTEBD method [29]. After the application of the single-site gates in $e^{-\mathrm{i}dt/2H_{\mathrm{ss}}}$, which are not unitary operators, we perform N_{corr} repetitions of a trivial time-evolution on both even and on odd bonds. This is done by applying two-body gates equal to the identity operator at the aim of keeping the MPS in canonical form. After each application of a two-body gate, we perform a singular value decomposition and a truncation step. We take only the $\chi_{\max}$ largest singular values, as long as these are larger than a truncation error $\varepsilon_{\mathrm{trunc}}$. We have observed that it is beneficial to have at least $N_{\mathrm{corr}} = 1$. This also relates to the fact that, after the application of the non-unitary gates, the entanglement in the MPS can decrease and the trivial evolution step can reduce the bond dimension while preparing the MPS for the two-body evolution. However, we also noticed that having $N_{\mathrm{corr}} > 1$ does not lead to further improvements. We mainly considered $N_{\mathrm{corr}} = 2$.

Concerning the truncation error $\varepsilon_{\mathrm{trunc}}$, this does not seem to be relevant in the phase where the dark state $|\mathrm{D_e}\rangle$ appears. Its precise value affects instead the transient dynamics in the phase related to state $|\mathrm{D}\rangle$. However, this is not expected to have impact on its fixed point. We explored values for the truncation error ranging from $\varepsilon_{\mathrm{trunc}} = 10^{-10}$ to $\varepsilon_{\mathrm{trunc}} = 10^{-14}$.

The results obtained with this iTEBD method are reported in Fig. 3(c). We furthermore mention here that the representative trajectories appearing in Fig. 1(c) have been obtained by simulating the stochastic quantum dynamics through MPSs and a TEBD method [28], for a finite chain with open boundary conditions.

Local coherence in the emergent dark state

In this section, we report the average value of the single-site coherence $\langle\lambda_4\rangle$ for the one-dimensional lattice. As shown in Fig. S1(b), coherence is present both in finite-size systems and in the thermodynamic limit, showing that the emergent dark state retains superposition of contagious and healthy states. Finally, we note that the fact that the approximation of the coherence (and of the order parameter) requires a non-trivial bond dimension in the whole phase demonstrates that the state is also entangled.

Average Lindblad dynamics

We have also simulated the open quantum dynamics of the average state ρ_t — which obeys the quantum master equation (1) — through MPS methods (see e.g. also Ref. [9] or Ref. [23] for an application to $2D$ dissipative systems). The idea is to represent the density matrix ρ_t as a vector $|\rho_t\rangle$ in an enlarged Hilbert space. This is achieved through the mapping

$$\rho = \sum_{\vec{\alpha},\vec{\beta}} r_{\vec{\alpha}\vec{\beta}}\,|\vec{\alpha}\rangle\langle\vec{\beta}| \to |\rho\rangle = \sum_{\vec{\alpha},\vec{\beta}} r_{\vec{\alpha}\vec{\beta}} \bigotimes_{k=1}^{N} \left(|\alpha_k\rangle \otimes |\beta_k\rangle\right)^{(k)}\,,$$

where $\vec{\alpha} = (\alpha_1, \alpha_2, \ldots \alpha_N)$ is a vector specifying the single-particle state of the different sites for the many-body state $|\vec{\alpha}\rangle$ and $r_{\vec{\alpha}\vec{\beta}} = \langle\vec{\alpha}|\,\rho\,|\vec{\beta}\rangle$.

In this representation, our Lindblad generator $\mathcal{L}$ becomes the following matrix

$$L = \gamma \sum_{k=1}^{N} \left(J^{(k)} - \frac{1}{2}\hat{n}_{*,\mathrm{I}}^{(k)} - \frac{1}{2}\hat{n}_{*,\mathrm{II}}^{(k)} \right) + \sum_{k=1}^{N} \Omega_1 \left(-\mathrm{i}\lambda_{1,\mathrm{I}}^{(k)} + \mathrm{i}\lambda_{1,\mathrm{II}}^{(k)} \right) + \\ - \mathrm{i} \sum_{k=1}^{N-1} \frac{\Omega_2}{2} \left(n_{\bullet,\mathrm{I}}^{(k-1)} + n_{\bullet,\mathrm{I}}^{(k+1)} \right) \lambda_{6,\mathrm{I}}^{(k)} + \mathrm{i} \sum_{k=1}^{N-1} \frac{\Omega_2}{2} \left(n_{\bullet,\mathrm{II}}^{(k-1)} + n_{\bullet,\mathrm{II}}^{(k+1)} \right) \lambda_{6,\mathrm{II}}^{(k)} , \tag{S7}$$

where $J = J_- \otimes J_-$, $\hat{n}_{\alpha,\mathrm{I}} = n_\alpha \otimes \mathbf{1}_3$, $\hat{n}_{\alpha,\mathrm{II}} = \mathbf{1}_3 \otimes n_\alpha$, and $\mathbf{1}_3$ is the three-dimensional identity matrix. In addition we have $\lambda_{\alpha,\mathrm{I}} = \lambda_\alpha \otimes \mathbf{1}_3$ and $\lambda_{\alpha,\mathrm{II}} = \mathbf{1}_3 \otimes \lambda_\alpha^T$.

The dynamics is implemented through the equation

$$\frac{d}{dt} |\rho_t\rangle = L \, |\rho_t\rangle \ .$$

This can be formally integrated to obtain $|\rho_t\rangle = e^{tL} |\rho\rangle$, and, since the matrix L contains at most two-site interactions, this evolution can be approximated with the same iTEBD method discussed in the previous section. As initial state, we consider the density matrix $\rho = |\mathrm{U}\rangle\langle\mathrm{U}|$, represented through the vector

$$|\rho\rangle = \bigotimes_{k=1}^{N} \left(|\bullet\rangle|\bullet\rangle \right)^{(k)} \ .$$

The main difference with the algorithm used to simulate the time-evolution under H_{eff}, lies in the way expectation values are computed. In this case, to compute the expectation value of a quantum observable, we first need to define a vector representation of the identity operator in the enlarged Hilbert space. This is given by

$$|\mathrm{id}\rangle = \bigotimes_{k=1}^{N} |\mathrm{id}_1\rangle^{(k)} \ ,$$

where $|\mathrm{id}_1\rangle = |\bullet\rangle|\bullet\rangle + |*\rangle|*\rangle + |\circ\rangle|\circ\rangle$ is the vector representation of the single-site identity operator. Expectation values are then computed as

$$\langle O^{(k)} \rangle_t = \langle \mathrm{id}| \, O_{\mathrm{L}}^{(k)} \, |\rho_t\rangle \ ,$$

with $O_{\mathrm{L}} = O \otimes \mathbf{1}_3$.

In the subcritical region — the one associated with the exact dark state $|\mathrm{D}\rangle$ — we have observed a good convergence of iTEBD results when increasing the bond dimension $\chi_{\max}$ of the MPS representation of $|\rho_t\rangle$. On the other hand, for large values of Ω_2/Ω_1, for which the system is expected to belong to the emergent dark state phase, it was not possible to obtain convergence of the iTEBD results, as the algorithm showed instabilities.

For $\Omega_2 \gg \Omega_1$, where the system features values of $\varrho_\bullet$ close to one, the state of the system is close to the product state with all sites in $|\bullet\rangle$. In this regime, far from the critical point, augmented product-ansatz descriptions — also known as augmented mean-field description — able to account for the weak short-ranged correlations in the state are expected to capture the relevant properties of the state (see e.g. Ref. [24] for an application to open quantum systems). In our numerical simulations, we have noted that the curves obtained with small bond dimensions ($\chi_{\max} = 4, 8$) are stable and provide a similar prediction for the steady-state value of $\varrho_\bullet$. Since even with a very small bond dimension, the MPS ansatz can account for short-ranged correlations beyond mean-field theories, we can regard such results as obtained from an augmented product-state description. This approach essentially provides an efficient version of standard perturbation theory. Indeed, it allows us to gradually include short-range correlations in the emergent dark state in a way which goes beyond a perturbative approach. It does not account for correlations at different orders in Ω_1, but it rather allows, in principle, to approximate correlations at all orders in Ω_1 within the correlation length allowed by the bond dimension.

The data obtained for these small bond dimensions are plotted in Fig. 3(c). These are in agreement with the results obtained for the effective Hamiltonian. This suggests that the steady state of the Lindblad dynamics is indeed the emergent dark state of H_{eff} in the supercritical region — the one associated with the emergent dark state $|\mathrm{D_e}\rangle$.

REPRESENTATION OF THE EFFECTIVE HAMILTONIAN IN THE FULLY SYMMETRIC SUBSPACE

To develop a representation of the Hamiltonian $H_{\rm eff}$ for the infinite-dimensional lattice in the fully symmetric subspace, it is convenient to use all the relevant Gell-Mann matrices λ_i, for $i = 1, 2, \dots 8$. Their algebraic structure is encoded in the commutation relations

$$[\lambda_i, \lambda_j] = 2i \sum_{\ell=1}^{8} \epsilon_{ij\ell} \lambda_\ell \,; \tag{S8}$$

importantly, $\epsilon_{ij\ell}$ is an anti-symmetric tensor. We further define the matrices $f_i = \frac{1}{2}\lambda_i$.

In order to efficiently represent the Hamiltonian, we need to derive a representation for collective operators constructed as

$$F_i = \sum_{k=1}^{N} f_i^{(k)} \,, \tag{S9}$$

as acting on fully symmetric states. For these operators, the commutation relations are inherited from Eq. (S8)

$$[F_i, F_j] = \sum_{k,h=1}^{N} \frac{1}{4} \left[\lambda_i^{(k)}, \lambda_j^{(h)}\right] = \sum_{k=1}^{N} \frac{1}{4} \left[\lambda_i^{(k)}, \lambda_j^{(k)}\right] = i \sum_{\ell=1}^{8} \epsilon_{ij\ell} F_\ell \,. \tag{S10}$$

Exploiting the anti-symmetric property of the tensor ϵ_{ijk}, it is possible to show that the operator

$$C = \sum_{i=1}^{8} F_i^2 \,,$$

is the (quadratic) Casimir operator for the algebra formed by the operators F_i, as it commutes with each of them. Indeed, one has that

$$[C, F_j] = \sum_{i=1}^{8} \left(F_i [F_i, F_j] + [F_i, F_j] F_i\right) = i \sum_{i,\ell=1}^{8} \epsilon_{ij\ell} \left(F_i F_\ell + F_\ell F_i\right) \,,$$

and looking at the last relation in the above equation, one sees that the term in the round brackets is symmetric with respect to exchange of $i \leftrightarrow \ell$, while the term $\epsilon_{ij\ell}$ is anti-symmetric. As such the total double sum is zero.

Because of this, the value of the Casimir operator in the fully symmetry sector could be computed by considering any state in the subspace, for instance also the state

$$|\mathrm{U}\rangle = \bigotimes_{k=1}^{N} |\bullet\rangle^{(k)} \,, \qquad \text{where} \qquad |\bullet\rangle = \begin{pmatrix} 1 \\ 0 \\ 0 \end{pmatrix} \,.$$

To make progress in finding a representation for the operators in Eqs. (S9), we now introduce a new set of operators, forming the so-called Cartan-Weyl basis, which are constructed from the F_i as follows:

$$I_\pm = F_1 \pm i F_2 \,, \quad I_3 = F_3 \,, \quad V_\pm = F_4 \pm i F_5 \,, \quad U_\pm = F_6 \pm i F_7 \,, \quad Y = \frac{2}{\sqrt{3}} F_8 \,. \tag{S11}$$

The commutation relations between these operators can be computed from the fundamental ones in Eq. (S10). We notice that $[I_3, Y] = 0$, so that these two operators can be simultaneously diagonalized. We define the normalized eigenstates of both I_3 and Y to be $|t, y\rangle$. In particular, we have

$$I_3 \, |t, y\rangle = t \, |t, y\rangle \,, \qquad Y \, |t, y\rangle = y \, |t, y\rangle \,.$$

Basically, we have that $t = (N_\bullet - N_*)/2$, where N_α denotes the total number of particles in state $|\alpha\rangle$, with $\alpha = \bullet, *, \circ$, and that $y = N_\bullet/3 + N_*/3 - 2N_\circ/3$. As such, $-N/2 \leq t \leq N/2$ and $-2N/3 \leq y \leq N/3$. This set of states forms a complete orthonormal basis for the subspace of interest.

For the vectors $|t, y\rangle$, the operators $I_\pm, V_\pm, U_\pm$ act as ladder operators. As a simple example of this fact, lets consider the state $|\mathrm{U}\rangle$ which can be written as $|\mathrm{U}\rangle = |N/2, N/3\rangle$. This is annihilated by the action of I_+, which wants to bring a particle from $|*\rangle$ to $|\bullet\rangle$. On the other hand, we have

$$I_- |N/2, N/3\rangle = \alpha |N/2 - 1, N/3\rangle \ ,$$

where α has to be determined through the norm of $I_- |N/2, N/3\rangle$. Using that I_+ annihilates $|\mathrm{U}\rangle$ we have that

$$\langle N/2, N/3| I_+ I_- |N/2, N/3\rangle = \langle N/2, N/3| [I_+, I_-] |N/2, N/3\rangle = N \, . \tag{S12}$$

So in this case, $\alpha = \sqrt{N}$.

In order to find the appropriate values of α for any state onto which I_- is acting, i.e. the value of α for generic

$$I_- |t, y\rangle = \alpha |t - 1, y\rangle \ ,$$

we need to develop a systematic approach. Lets focus for the moment on the subalgebra formed by $I_\pm$ and I_3. These operators are made of the sum of 3×3 matrices which basically represent the spin-1/2 algebra (the algebra of Pauli matrices) embedded into a largest (3×3) space. This can also be seen by noticing that $I_\pm$ and I_3 have among them the same commutation relations of spin-1/2 operators. We then compute

$$I_+ I_- = F_1^2 + F_2^2 + i[F_2, F_1] = \left[F_1^2 + F_2^2 + F_3^2\right] - F_3(F_3 - 1) \, .$$

The operator in the square brackets is a "partial" Casimir operator, which we call $C_{12} = \sum_{i=1}^{3} F_i^2$, since it commutes with the subalgebra formed by the F_i, with $i = 1, 2, 3$. As such, C_{12} also commutes with the $I_\pm$. As apparent from Eq. (S12), it is important to understand the value of this operator on different states in order to be able to compute the norm of vectors such as $I_- |t, y\rangle$.

Since C_{12} commutes with $I_\pm$ and that $I_\pm$ does not modify y, to find the value of this partial Casimir operator C_{12} in the different subspaces (labelled by the value of y), it is convenient to find a simple state to compute its expectation value. In particular, we look for the one which has the maximum value of t allowed, for a fixed value of y (and given that we have only N particles). We call $N_{\bullet *}$ the number of particles which are in state $|\bullet\rangle$ or $|*\rangle$. We thus have $N_{\bullet *} + N_\circ = N$ and also that, given a value of $\bar{y}$ we have

$$\bar{y} = \frac{N_{\bullet *} - 2N_\circ}{3} \, , \longrightarrow N_{\bullet *} = \bar{y} + \frac{2N}{3} \, .$$

Then, if all the particles in the subspace formed by the states $|\bullet\rangle, |*\rangle$ are found in the state $|\bullet\rangle$ we have the maximum

$$t_{\max|\bar{y}} = \frac{N_{\bullet *}}{2} = \frac{\bar{y} + \frac{2N}{3}}{2} \, .$$

We can thus find the value of the partial Casimir operator C_{12}, at fixed $\bar{y}$, which is given by

$$\langle t_{\max|\bar{y}}, \bar{y}| C_{12} |t_{\max|\bar{y}}, \bar{y}\rangle = \frac{N_{\bullet *}}{2} \left(\frac{N_{\bullet *}}{2} + 1\right) = \left(\frac{\bar{y} + \frac{2N}{3}}{2}\right) \left(\frac{\bar{y} + \frac{2N}{3}}{2} + 1\right) \, .$$

With this result, we can now find all matrix elements for the operator I_-, in the fully symmetric subspace. Indeed, we use that

$$I_- |t, y\rangle = \alpha_{t,y} |t - 1, y\rangle \ , \tag{S13}$$

where $\alpha_{t,y}^2$ is given by

$$\alpha_{t,y}^2 = \langle t, y| I_+ I_- |t, y\rangle = \langle t, y| C_{12} - I_3(I_3 - 1) |t, y\rangle = t_{\max|y} \left(t_{\max|y} + 1\right) - t\,(t - 1) \, .$$

Now we use an analogous procedure to represent the ladder operator U_-. The action of U_- on a state consists in taking one particle from state $|*\rangle$ and bringing it to state $|\circ\rangle$. This means that the action of U_- reduces y by 1 but also increments t by 1/2. We thus have the relation

$$U_- |t, y\rangle = \beta_{t,y} |t + \frac{1}{2}, y - 1\rangle \ ; \tag{S14}$$

Similarly to what done before, the factor $\beta^2_{t,y}$ can be written as

$$\beta^2_{t,y} = \langle t,y| U_+U_- |t,y\rangle = \langle t,y| \left[C_{23} - \tilde{F}_8\left(\tilde{F}_8 - 1\right)\right] |t,y\rangle \ ,$$

where

$$\tilde{F}_8 = \sum_{k=1}^{N} \frac{1}{4}\left(\sqrt{3}\lambda_8 - \lambda_3\right)^{(k)} \ ,$$

while $C_{23} = F_6^2 + F_7^2 + \tilde{F}_8^2$ is the partial Casimir operator, now for the subspace generated by $|*\rangle, |\circ\rangle$. We note that $\tilde{F}_8 = \frac{3}{4}Y - \frac{1}{2}I_3$. The task is to find a way to compute the value of this partial Casimir operator on a simple reference state. We proceed as follows. Lets consider a generic state $|t,y\rangle$, and remember that we have N particles. We thus can find

$$2t = N_\bullet - N_* \quad y = N_\bullet + N_* - \frac{2N}{3} \, . \tag{S15}$$

Inverting the above relations, we can find an expression for $N_\bullet, N_*$ (and thus also for $N_\circ$ if necessary) as a function of t, y. We have

$$N_\bullet = t + \frac{y}{2} + \frac{N}{3} \, , \qquad N_* = \frac{y}{2} - t + \frac{N}{3} \, .$$

As already said, the action of the operator U_- is that of taking one particle from $|*\rangle$ and bringing it to $|\circ\rangle$. As such, without changing the value of the partial Casimir operator (since $[U_-, C_{23}] = 0$), this state is connected by the repeated action of U_- to the state with $N_\bullet = t + \frac{y}{2} + \frac{N}{3}$ as before, $N_* = 0$ and $N_\circ = N - N_\bullet$. Such a state is given by

$$|\varphi\rangle = |\frac{t}{2} + \frac{y}{4} + \frac{N}{6}, t + \frac{y}{2} - \frac{N}{3}\rangle \ ,$$

and, from this, the partial Casimir operator C_{23} can be computed solely as a function of t, y of the original state. In particular, we have

$$\langle\varphi| C_{23} |\varphi\rangle = \frac{N_\circ}{2}\left(\frac{N_\circ}{2} + 1\right) = \frac{1}{2}\left(\frac{2N}{3} - t - \frac{y}{2}\right)\left[\frac{1}{2}\left(\frac{2N}{3} - t - \frac{y}{2}\right) + 1\right] \ ,$$

and, therefore,

$$\beta^2_{t,y} = C_{23} - \left[\frac{3}{4}y - \frac{t}{2}\right]\left[\frac{3}{4}y - \frac{t}{2} - 1\right] \, .$$

This procedure allows us to represent the effective Hamiltonian in Eq. (S1), in the fully symmetric subspace spanned by all vectors $|t,y\rangle$. Using relations (S13) and (S14), we indeed have

$$I_- = \sum_{t,y} \alpha_{t,y} |t-1,y\rangle \langle t,y| \ ,$$

and

$$U_- = \sum_{t,y} \beta_{t,y} |t + \frac{1}{2}, y-1\rangle \langle t,y| \ .$$

We can use this to represent the effective Hamiltonian noticing that

$$\sum_{k=1}^{N} \lambda_1^{(k)} = I_- + I_+ \, ,$$

and also that

$$\sum_{k=1}^{N} \lambda_6^{(k)} = U_- + U_+ \, .$$

Furthermore, we also have

$$\sum_{k=1}^{N} n_{\bullet}^{(k)} = I_3 + \frac{Y}{2} + \frac{N}{3}\,,$$

and

$$\sum_{k=1}^{N} n_{*}^{(k)} = -I_3 + \frac{Y}{2} + \frac{N}{3}\,.$$

We have used this representation of the Hamiltonian to produce numerical data for the plots presented in Fig. 2(c-d) as well as those shown in Fig. S2.

ADDITIONAL NUMERICAL RESULTS FOR THE INFINITE-DIMENSIONAL LATTICE

In this section, we present data showing that the gap of the H_{eff} Hamiltonian remains finite in the region $\Omega_2 < 2\Omega_1$ while it tends to zero for values of $\Omega_2 > 2\Omega_1$. At the critical point $\Omega_2 = 2\Omega_1$, we have instead a power-law decay of the gap with an exponent close to 0.31. All of this is shown in Fig. S2.

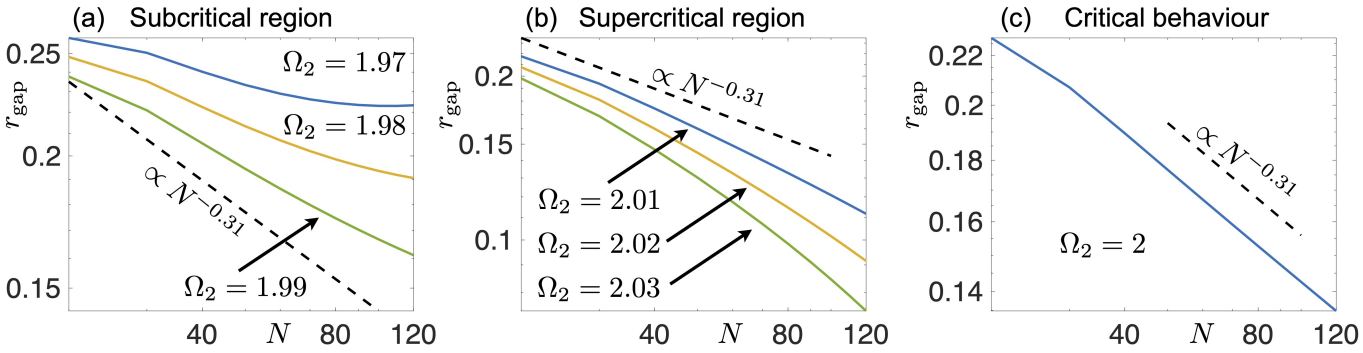

FIG. S2. **Gap of the effective Hamiltonian for the infinite-dimensional lattice**. Log-log plots of the gap r_{gap} of H_{eff} as a function of N in different parameter regimes for $\Omega_1 = 1$ (in units of γ). (a) In the subcritical region, identified by values of $\Omega_2 < 2\Omega_1$, the gap shows a tendency to saturate to a finite value. This is manifesting in the log-log plot via curves which are concave up. (b) In the supercritical region, instead we have that curves are concave down which indicates an exponential decay of the gap as a function of N. (c) At criticality, $\Omega_2 = 2\Omega_1$, the gap tends to vanish with a power-law behaviour, with an exponent approximately equal to -0.31. In all panels, the dashed line, proportional to $N^{-0.31}$, is shown for comparison.

PRACTICAL IMPLEMENTATION OF THE CONSTRAINT

In this section we provide details on the discussion about the possibility of implementing the constrained system Hamiltonian in experiments reported in the main text.

We consider an experimental setting involving several three-level Rydberg atoms, arranged in a $1D$ array. We take the following Hamiltonian

$$H_{\rm exp} = \Omega_1 \sum_k \lambda_1^{(k)} + \Omega_2 \sum_k \lambda_6^{(k)} + H_{\rm diag}\,, \tag{S16}$$

whose first two terms represent two laser drivings, while $H_{\rm diag} = \sum_k H_{\rm at}^{(k)}$, where $H_{\rm at}^{(k)}$ contains the interaction energy of a single atom associated with its configuration and that of its neighbors (the left one, L, and the right one, R) as well as laser detuning terms. For a reference atom, we have

$$H_{\rm at} = H_{\rm int} + H_{\rm det}\,, \qquad \text{with} \quad H_{\rm int} = \sum_{\alpha,\beta=\bullet,*,\circ}^{3} V_{\alpha\beta}(n_\beta^{(\rm L)} + n_\beta^{(\rm R)})n_\alpha\,, \quad H_{\rm det} = \sum_{\alpha=\bullet,*,\circ}^{3} h_\alpha n_\alpha\,. \tag{S17}$$

here, h_α are the detunings while the symmetric matrix $V_{\alpha\beta}$ encodes the state-dependent atomic interactions.

The main idea to obtain the desired constraint consists in "rotating" the system Hamiltonian $H_{\rm exp}$ into an interaction picture obtained by subtracting to the time-evolution, the unitary operator

$$U_t = \prod_k e^{-{\rm i}tH_{\rm at}^{(k)}}$$

In this frame, the Hamiltonian $H_{\rm exp}$ transforms into

$$H'_{\rm exp} = U_t^\dagger \left(\sum_k \Omega_1 \lambda_1^{(k)} + \Omega_2 \lambda_6^{(k)} \right) U_t\,. \tag{S18}$$

To explicitly write down such an operator, we need to evaluate the action of $e^{{\rm i}tH_{\rm at}}$ on the different states $|\circ\rangle, |*\rangle, |\bullet\rangle$. This is indeed enough to understand how the off-diagonal matrices λ_1 and λ_6 transform in the rotating frame. We will also apply a rotating wave approximation. Different choices of h_α and $V_{\alpha\beta}$ can thus give rise to different constraints. The first step is thus to compute the following expression ($\alpha = \bullet, *, \circ$):

$$\begin{aligned}\exp(iH_{\rm at}t)|\alpha\rangle = \exp\left(it \left[h_\alpha + \sum_{\beta=\bullet,*,\circ}^{3} V_{\alpha\beta}(n_\beta^{(\rm L)} + n_\beta^{(\rm R)}) \right] \right) |\alpha\rangle = \\ = \exp\left(ith_\alpha\right) \left[1 - \sum_\beta n_\beta^{(\rm L)} \left[1 - e^{itV_{\alpha\beta}}\right] \right] \left[1 - \sum_{\beta'} n_{\beta'}^{(\rm R)} \left[1 - e^{itV_{\alpha\beta'}}\right] \right] |\alpha\rangle\,.\end{aligned} \tag{S19}$$

The aim is to constrain the transition between states $|\circ\rangle$ and $|*\rangle$. To this end, we can choose $h_\bullet = h_* = 0$, as well as $V_{\alpha\beta}$ with non-zero components only given by $V_{\bullet\circ} = V_{\circ\bullet}$. In this way, by also fixing $h_\circ = -V_{\circ\bullet}$ and neglecting oscillating terms, we find

$$e^{iH_{\rm at}t}|*\rangle = |*\rangle \qquad e^{iH_{\rm at}t}|\circ\rangle \approx |\circ\rangle \left[n_\bullet^{(\rm L)} + n_\bullet^{(\rm R)} - 2n_\bullet^{(\rm L)} n_\bullet^{(\rm R)} \right],$$

and

$$e^{iH_{\rm at}t}|\bullet\rangle \approx |\bullet\rangle \left[\left(1 - n_\circ^{(\rm L)}\right) + \left(1 - n_\circ^{(\rm R)}\right) \right],$$

Using these results for the Hamiltonian in Eq. (S18) leads to the many-body operator

$$H'_{\rm exp} \approx \sum_k \left[\Omega_1 \left(1 - n_\circ^{(k-1)}\right) \left(1 - n_\circ^{(k+1)}\right) \lambda_1^{(k)} + \Omega_2 \left(n_\bullet^{(k-1)} + n_\bullet^{(k+1)} - 2n_\bullet^{(k-1)} n_\bullet^{(k+1)} \right) \lambda_6^{(k)} \right], \tag{S20}$$

which is the one reported in the main text.